



Flood Forecasting and Inundation Mapping Using HiResFlood-UCI and Near-Real-Time Satellite Precipitation Data: The 2008 Iowa Flood

PHU NGUYEN, ANDREA THORSTENSEN, SOROOSH SOROOSHIAN,
KUOLIN HSU, AND AMIR AGHAKOUCHAK

Department of Civil and Environmental Engineering, University of California, Irvine, Irvine, California

(Manuscript received 30 October 2014, in final form 20 January 2015)

ABSTRACT

Floods are among the most devastating natural hazards in society. Flood forecasting is crucially important in order to provide warnings in time to protect people and properties from such disasters. This research applied the high-resolution coupled hydrologic–hydraulic model from the University of California, Irvine, named HiResFlood-UCI, to simulate the historical 2008 Iowa flood. HiResFlood-UCI was forced with the near-real-time Precipitation Estimation from Remotely Sensed Information Using Artificial Neural Networks–Cloud Classification System (PERSIANN-CCS) and NEXRAD Stage 2 precipitation data. The model was run using the a priori hydrologic parameters and hydraulic Manning n values from lookup tables. The model results were evaluated in two aspects: point comparison using USGS streamflow and areal validation of inundation maps using USDA’s flood extent maps derived from Advanced Wide Field Sensor (AWiFS) 56-m resolution imagery. The results show that the PERSIANN-CCS simulation tends to capture the observed hydrograph shape better than Stage 2 (minimum correlation of 0.86 for PERSIANN-CCS and 0.72 for Stage 2); however, at most of the stream gauges, Stage 2 simulation provides more accurate estimates of flood peaks compared to PERSIANN-CCS (49%–90% bias reduction from PERSIANN-CCS to Stage 2). The simulation in both cases shows a good agreement (0.67 and 0.73 critical success index for Stage 2 and PERSIANN-CCS simulations, respectively) with the AWiFS flood extent. Since the PERSIANN-CCS simulation slightly underestimated the discharge, the probability of detection (0.93) is slightly lower than that of the Stage 2 simulation (0.97). As a trade-off, the false alarm rate for the PERSIANN-CCS simulation (0.23) is better than that of the Stage 2 simulation (0.31).

1. Introduction

Floods are among the most devastating natural hazards in terms of the number of people affected and economic loss (Ashley and Ashley 2008; Cook and Merwade 2009). Figure 1, which was produced using data from the Center for Research on the Epidemiology of Disasters (CRED; www.emdat.be), shows the worldwide flood statistics from 1950 to 2010. There was a significantly increasing trend in number of floods occurring, number of deaths, number of people affected, and economic damage over the past half century. In the 1990s, approximately 100 000 people died and 1.4 billion people were affected (Fig. 1) as a result of the severe floods that occurred in China. Between 1987 and 1997, 44% of all floods happened in

Asian countries, causing 288 000 deaths and economic damage of \$136 billion (U.S. dollars) (WMO 2011). In 2011, floods were the third-most severe cause of both deaths and damage costs for any natural hazard in the United States (National Weather Service 2012). Climate change leads to an increase in precipitation intensity in many parts of the world, which may cause more severe floods (Solomon et al. 2007).

The primary driver of a regular flood over a region is extreme rainfall, while other types of floods can be caused by dam breaks, high tides, and snow melting. Many efforts have been made from various organizations across the world to prevent/mitigate the impact of floods on society; however, modeling and forecasting floods caused by extreme precipitation, especially flash floods, is still very challenging (Borga et al. 2011). The difficulty exists with two main aspects: modeling techniques and data acquisition.

Hydrologic and hydraulic models have been used to model floods driven by rainfall data from various

Corresponding author address: Phu Nguyen, Dept. of Civil and Environmental Engineering, E/4130 Engineering Gateway, Office EH 5308, Mail Code 2175, Irvine, CA 92697.
E-mail: ndphu@uci.edu

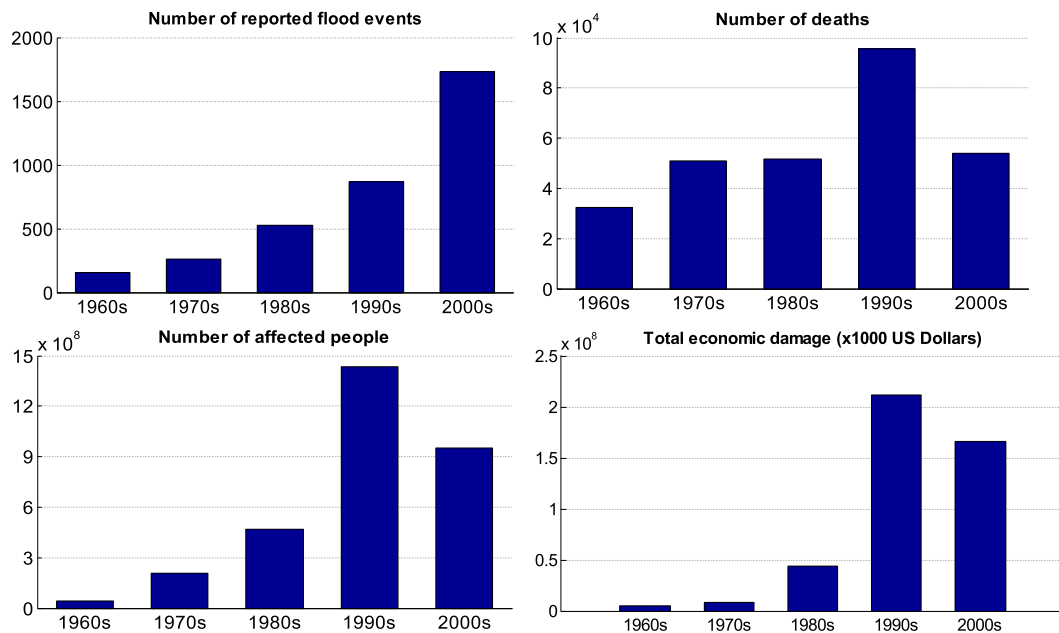


FIG. 1. Flood statistics from 1950 to 2010 using data from CRED.

sources: gauges, radars, satellites, and numerical forecast models. Gauge rainfall data can be the most reliable as “true observation,” but it is “point” data and difficult to extrapolate over a relatively large area (Collier 2007). Further, the gauge observation network is neither dense enough nor uniform in global scale, especially in rural, mountainous areas where floods occur more often. Radars have been used to estimate precipitation for flood warnings, but they are expensive to operate and their coverage is also limited, particularly in mountainous regions (Sorooshian et al. 2014).

Remote sensing technologies have come up since the 1960s (Jensen 2000) as having the greatest potential for near-real-time precipitation estimation in global-scale flood warnings with high resolution (i.e., 4 km). The recently developed satellites by NASA [i.e., Tropical Rainfall Measuring Mission (TRMM)], NOAA [Geostationary Operational Environmental Satellite (GOES)], and other international organizations offer great opportunities for developing global flood warning systems. Those systems include the Global Flood and Landslide Monitoring system by NASA (Hong et al. 2007a), the Global Flash Flood Guidance System (GFFGS) developed by the U.S. Hydrologic Research Center, the Global Flood Alert System (GFAS) developed in Japan by the International Centre for Water Hazard and Risk Management under the auspices of the United Nations Educational, Scientific, and Cultural Organization (ICHARM; www.icharm.pwri.go.jp/research/ifas/), and the Global Flood Monitoring System (<http://flood.umd.edu/>) by the University of Maryland (Wu et al. 2014). All

the systems use hydrologic models at kilometer resolutions with or without one-dimensional routing schemes forced with satellite precipitation data to provide basic warnings on where there is the potential for floods to occur. None of them can show the details of the floods, for example, spatiotemporal distribution of water depth and flow velocity at river scale, which are crucially important in flood analysis and warnings.

Together with the rapid evolution in remote sensing technologies, more data with larger coverage and finer spatiotemporal resolution have been available for use. Furthermore, with numerous contemporary and future missions such as NASA’s Global Precipitation Measurement (GPM; launched in 2014) and NASA’s Soil Moisture Active Passive (SMAP; launched in 2015), NASA offers the unique opportunity to better understand the physics of floods in order to develop a new generation of models, which will improve global flood forecasting. Moreover, powerful computing systems motivate modelers to use high-resolution hydrologic–hydraulic models to simulate the water flow in rivers and flood plains as realistically as possible to protect people and mitigate the damages of their properties caused by extreme flood hazards.

Satellite-based surface water measurements have been widely used in flood observation and forecasting. Information from satellite sensors such as the Landsat Thematic Mapper (TM), Advanced Wide Field Sensor (AWIFS), Moderate Resolution Imaging Spectroradiometer (MODIS), Advanced Synthetic Aperture Radar (ASAR), Advanced Microwave Scanning Radiometer for Earth Observing System (AMSR-E), and Ocean

Topography Experiment (TOPEX)/Poseidon radar altimeter can be used to estimate flood inundation, water level, and river discharge. Applications of satellite-based surface water measurements can be found in Hossain et al. (2014a,b), Khan et al. (2014), Alsdorf et al. (2007), Bjerkli et al. (2005), Brakenridge et al. (2007), Bates et al. (1997), and Behrangi et al. (2011). The near-real-time (NRT) Global Flood Mapping system recently developed by NASA for near-real-time global flood monitoring and its archived data will be a great resource for validating the proposed system (<http://oas.gsfc.nasa.gov/floodmap>). NASA's Surface Water Ocean Topography (SWOT; to be launched in 2020) will provide global river discharge observation (Wu et al. 2014), which is promised to be a revolutionary resource for flood observation and forecasting in addition to validation of flood modeling at a global scale.

The Iowa Flood Center (IFC) hosted a NASA GPM validation field campaign in the spring of 2013 known as Iowa Flood Studies (IFloodS). The focus of the IFloodS campaign was to explore advantages and weaknesses of satellite precipitation products in terms of their application toward understanding and forecasting hydrologic processes (Krajewski et al. 2013).

This paper presents an application of the recently developed high-resolution coupled hydrologic–hydraulic model from the University of California, Irvine (HiResFlood-UCI; Nguyen et al. 2012, 2013) with near-real-time satellite precipitation data [Precipitation Estimation from Remotely Sensed Information Using Artificial Neural Networks–Cloud Classification System (PERSIANN-CCS)] for flood forecasting and inundation mapping in the Cedar River in Iowa. The system was validated for the historical 2008 Iowa flood event using U.S. Department of Agriculture (USDA) flood extent maps derived from the high-resolution AWIFS imagery and observations from U.S. Geological Survey (USGS) streamflow gauges along the main channel of the Cedar River. The modeling framework uniquely integrates areal imagery into a coupled hydrologic–hydraulic modeling framework and offers a unique avenue for validation and verification of inundation models. This work aims to supplement the efforts of the IFloodS campaign through application of HiResFlood-UCI to a major flood event within the IFloodS domain. The application is done in the context of using near-real-time satellite precipitation data in a forecasting environment.

2. HiResFlood-UCI

HiResFlood-UCI is a high-resolution coupled hydrologic–hydraulic model based on the heritage of the National Weather Service's Hydrology Laboratory

Research Distributed Hydrologic Model (HL-RDHM; National Weather Service 2011) and BreZo (Begnudelli and Sanders 2006) for hydraulic flood modeling (inundation mapping, flow depth, and velocity estimation) purposes.

Detailed description of HL-RDHM can be found in Koren et al. (2004) and National Weather Service (2011). HL-RDHM is a distributed hydrologic model that was designed and implemented for the entire contiguous United States (CONUS) at three spatial resolutions of 1 Hydrologic Rainfall Analysis Project (HRAP; ~4 km), 1/2 HRAP, and 1/4 HRAP. HL-RDHM structure can also be applied for any cell resolution and time step length. The heart of HL-RDHM is the Sacramento Soil Moisture Accounting (SAC-SMA) rainfall–runoff model. In SAC-SMA, unlike other distributed models with fixed values for subdomains or the entire domain, an advanced algorithm was designed to derive *a priori* parameters from soil and land use data.

BreZo is a hydraulic model that solves the shallow-water equations using a Godunov-type finite volume method with an unstructured grid of triangular cells. A detailed description of the model can be seen in Begnudelli and Sanders (2006). One of the primary advances of the model is that it was designed for working with an unstructured grid of triangular cells, which enables the model to simulate the water flow in varying shapes of the channel–river systems. The model has been applied successfully to simulate dam breaks and flood inundation (Begnudelli and Sanders 2007; Sanders 2007).

The coupled model uses HL-RDHM as a rainfall–runoff generator and replaces the routing scheme of HL-RDHM with the 2D hydraulic model (BreZo) for providing more detailed information of flooding at river scale, for example, flood depths, flooded maps, and flow velocity, which are essential for improved flood warnings. A semiautomated technique of unstructured mesh generation using Triangle software (Shewchuk 1996) and Esri ArcGIS was developed for the hydraulic component of HiResFlood-UCI. Such mesh has a high resolution at decameters in areas along the river network and coarse resolution for the rest of the simulation domain, in order to simulate flooded areas in detail while keeping the computational costs to a bare minimum. HiResFlood-UCI can be run using either calibrated parameters for areas with streamflow observation available or the *a priori* hydrologic parameters for the CONUS from the NWS and hydraulic Manning *n* values from lookup tables. The model was successfully implemented for Baron Fork at Eldon, OK (ELDO2), one of the catchments in the Distributed Model Intercomparison Project, phase 2 (DMIP 2; Nguyen et al. 2012), and the upper Little

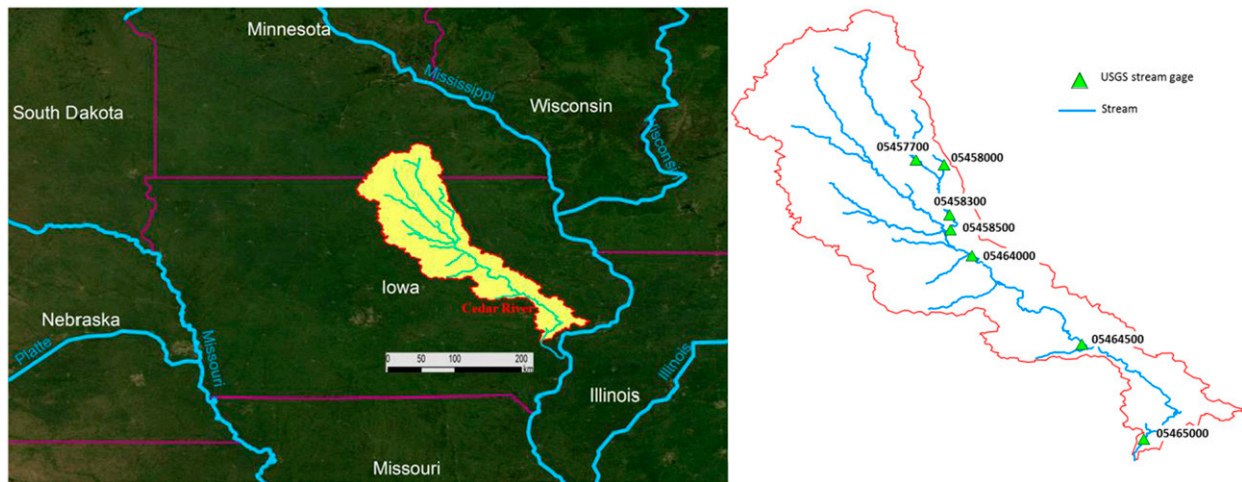


FIG. 2. Cedar River watershed, USGS streamflow gauge IDs, and locations in the Cedar River watershed used for validation.

Missouri River for simulating the historical flash flood event in June 2010 (Nguyen et al. 2013).

3. Near-real-time satellite precipitation PERSIANN-CCS

PERSIANN-CCS (Hong et al. 2004) is a near-real-time satellite precipitation product. Precipitation is estimated by algorithms developed by the scientists at the Center for Hydrometeorology and Remote Sensing (CHRS) at the University of California, Irvine. The product has high spatiotemporal resolution at hourly, $0.04^\circ \times 0.04^\circ$, quasi-global coverage from 60°N to 60°S . PERSIANN-CCS algorithms estimate precipitation from geosynchronous Earth orbit infrared (GEO-IR) imagery using artificial neural networks (ANNs) and cloud classification system techniques. More detailed descriptions on the development of PERSIANN-CCS algorithms, product validation, and application can be found in Hsu et al. (1997, 2013), Sorooshian et al. (2000), and Hong et al. (2004, 2007b). Since PERSIANN-CCS is available in near-real time with about a 1-h delay, it is suitable for use in providing flood warnings to the public and flood disaster managers (Sorooshian et al. 2014; Nguyen et al. 2014). This is particularly true for larger river systems, such as the Cedar River, where the 1-h time latency has much less of an impact on lead time compared to smaller rivers and those prone to flash floods.

4. Implementing HiResFlood-UCI with PERSIANN-CCS data for Cedar River

a. Domain and data used

The Cedar River is a 544-km river in Minnesota and Iowa with a drainage area of approximately $20\,000\text{ km}^2$

(Fig. 2). The Cedar River flows through two major cities (Waterloo and Cedar Rapids) in Iowa. Agriculture is the main land use in the Cedar River basin (Linhart and Eash 2010).

The digital elevation model (DEM) at 30-m resolution with vertical accuracy of $\pm 2.44\text{ m}$ in root-mean-square error (RMSE) was downloaded from USGS's National Hydrology Dataset (NHD). Near-real-time global PERSIANN-CCS precipitation data at 0.04° resolution are retrieved from the CHRS's server. The original PERSIANN-CCS is in geographical projection (latitude-longitude), so it is necessary to convert the data to the HRAP using the code provided by the NWS (available at www.nws.noaa.gov/oh/hrl/dmip/lat_lon.txt) for HiResFlood-UCI.

b. Model setup

HiResFlood-UCI was set up for the Cedar River watershed following the procedure in Nguyen et al. (2014). HL-RDHM was set at an hourly time step, 1-HRAP resolution. HL-RHDM was implemented with the a priori parameters (Koren et al. 2003) from NWS and had a spinup period of over 2 yr (starting in early 2006) leading up to the major flooding period. The hydraulic component, BreZo, was run beginning a month prior to the main flood. This time period incorporated several precipitation events that preceded the major flood and allowed for the channels in the model to reach initial flow conditions.

From USGS 30-m DEM, Cedar River watershed was delineated into 29 subcatchments using ArcGIS terrain processing tools (Fig. 3). The unstructured triangular mesh was designed using Triangle software (Shewchuk 1996) with buffering sizes and area constraints described in detail in Table 1. The highest resolution along the

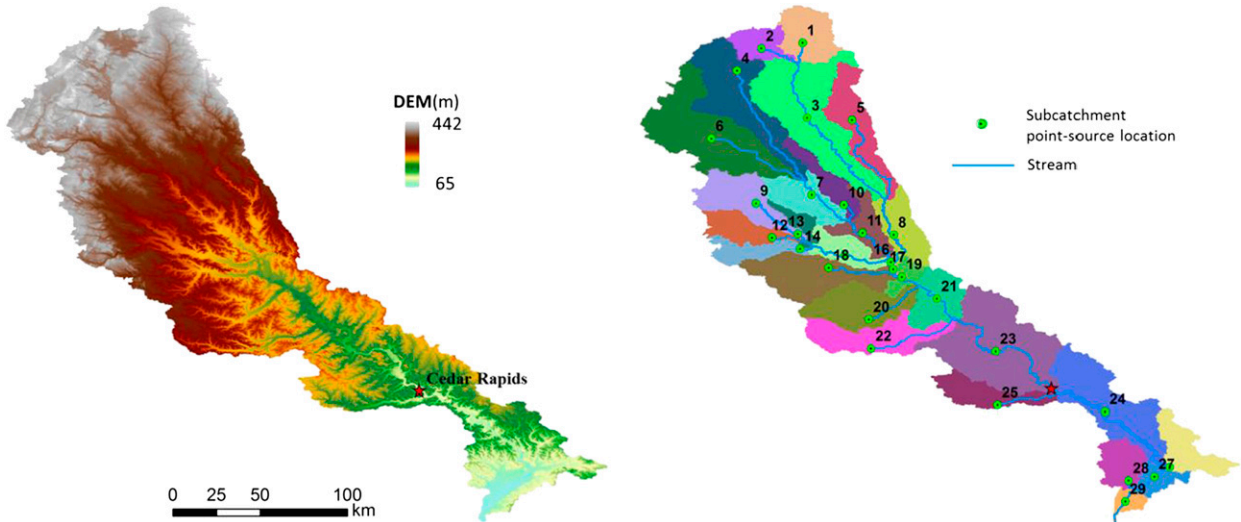


FIG. 3. The 30-m DEM and watershed delineation results including streams, subcatchments, and point-source locations.

river network and within 100 m from the river center line is 30 m. Manning n values for the channel and floodplain of Cedar River were selected from Chow's lookup table (Chow 1959) at 0.045 and 0.060, respectively.

5. Application of the model for simulating the 2008 Iowa flood

a. Description of the 2008 Iowa flood

A sweep of several storms associated with sequential frontal system passages over the midwestern United States was the primary contributor to the historic 2008 flood. The state of Iowa averaged 167 mm of rain above normal for the period from 29 May to 12 June. This occurred following an unusually heavy snowpack during the winter of 2007/08, which provided enough snowmelt to saturate soils and elevate river levels prior to the arrival of the late spring storms.

The 2008 flood is the largest flood on record for the Cedar River basin, and it had a peak discharge representing a 0.2%–1% annual recurrence at the Cedar River stream gauge near the outlet (Linhart and Eash 2010). The streamflow measured by USGS's stream gauge on the Cedar River at Cedar Rapids reached to $3964 \text{ m}^3 \text{s}^{-1}$, twice the maximum record of 110 yr (Smith et al. 2013).

b. Data collection

Precipitation from PERSIANN-CCS from 29 May to 25 June 2008 was collected to use as forcing data in the simulation. Additionally, real-time hourly gridded radar-estimated precipitation with no bias removal (4 km) NEXRAD Stage 2 or "RAD" data for the same time period was obtained from the University Corporation

for Atmospheric Research (UCAR; <http://data.eol.ucar.edu/codiac/dss/id=21.006>) for a comparison to the satellite product. The real-time hourly digital precipitation (HDP) radar data in this Stage 2 product were estimated by the WSR-88D product generator at the National Centers for Environmental Prediction (NCEP). Stage 2 rainfall data were selected for comparison because they are also real-time products that could be used in a forecasting setting (albeit limited to the United States). Figure 4 shows a side-by-side comparison of precipitation totals for the 2008 flood event for both products. Overall, both products exhibit similar precipitation total patterns, with the PERSIANN-CCS producing less precipitation than Stage 2. It can be seen that both products have an area of maximum total precipitation located upstream of the Cedar Rapids area, where the most damaging flooding in the basin occurred. The total basin average precipitation during the 2008 flood event for PERSIANN-CCS was 378.89 mm and for Stage 2 was 458.89 mm.

Using the Stage 2 precipitation as a baseline, spatial statistics were calculated between PERSIANN-CCS and Stage 2. Figure 5 highlights these spatial relationships. The highest RMSE is found in the central basin, which

TABLE 1. Mesh design for BreZo.

Buffer zone	Distance from river (m)	Mesh resolution	
		Size (m)	Area (m^2)
1	100	30	450
2	500	50	1250
3	1000	100	5000
4	5000	500	125 000
5	20 000	1000	500 000

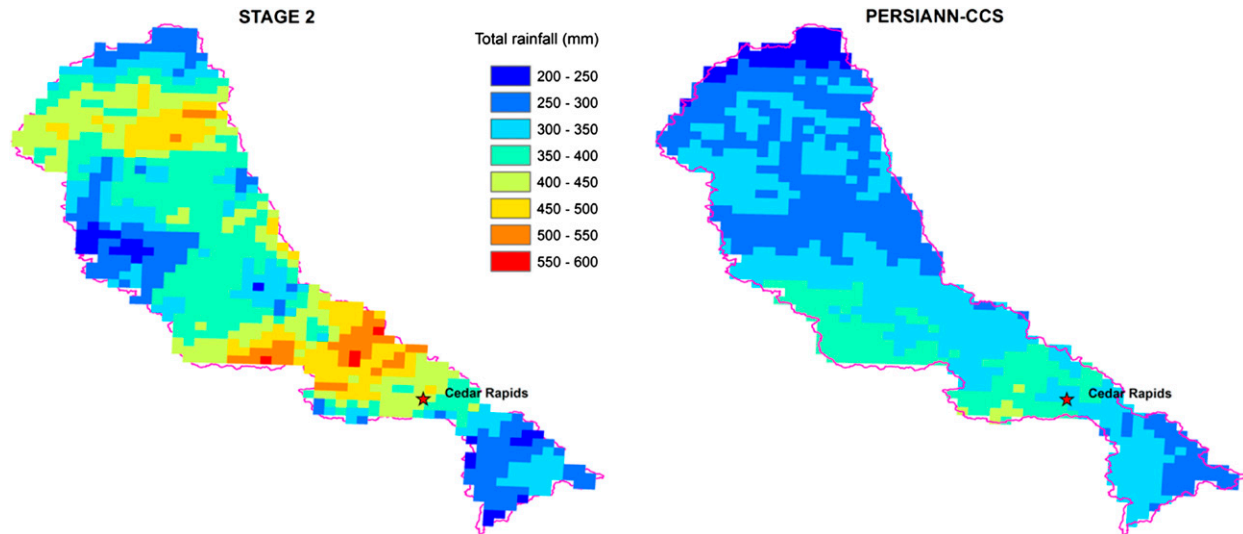


FIG. 4. Total precipitation during the event from 0000 UTC 29 May to 2300 UTC 25 Jun 2008: Stage 2 and PERSIANN-CCS.

coincides with the location of the maximum total precipitation band. Areas with the highest positive biases are detected in the southern and western regions of the basin, and areas with the strongest negative biases are exhibited throughout the northern and central basin. The correlation coefficient pattern closely mimics that of RMSE, with the lowest correlation being in the central basin.

Observations from seven USGS streamflow gauges scattered across the basin were used to analyze the simulated hydrographs produced by HiResFlood-UCI. Locations and identifications (IDs) of these gauges are shown in Fig. 2.

This research used the AWIFS flood extent data from the USDA. Johnson and Lindsey (2008) suggest AWIFS (56-m resolution) as an excellent compromise between Landsat (30-m resolution but not frequent enough) and MODIS (250-m resolution but more frequent). AWIFS imagery is taken from the AWIFS sensor on board the *Indian Remote Sensing Satellite (IRS-P6)*. AWIFS

imagery has 56-m resolution at nadir with a swath of 740 km and a 5-day revisit (Indian National Remote Sensing Agency 2003). AWIFS imagery has been successfully incorporated into other USDA applications with high-resolution requirements, particularly agriculture monitoring (Boryan et al. 2011). The AWIFS images over the Iowa area on 29 May and 16 June 2008 were classified into flood/nonflood and then converted into vector format (shapefile) by USDA. The data in shapefile format were downloaded from the USGS Hazards Data Distribution System (HDDS; <http://hddsexplorer.usgs.gov/data>). Fig. 6 illustrates the magnitude of the 2008 Iowa flood in the Cedar River basin as seen by AWIFS.

As the figure shows, most of the basin's streamflow conditions are characterized with these images, except the northern-most upstream segment is not fully covered. This was of little concern, as the most impacted area is the river toward the southern half of the basin, particularly near the Cedar Rapids area. This preclassified

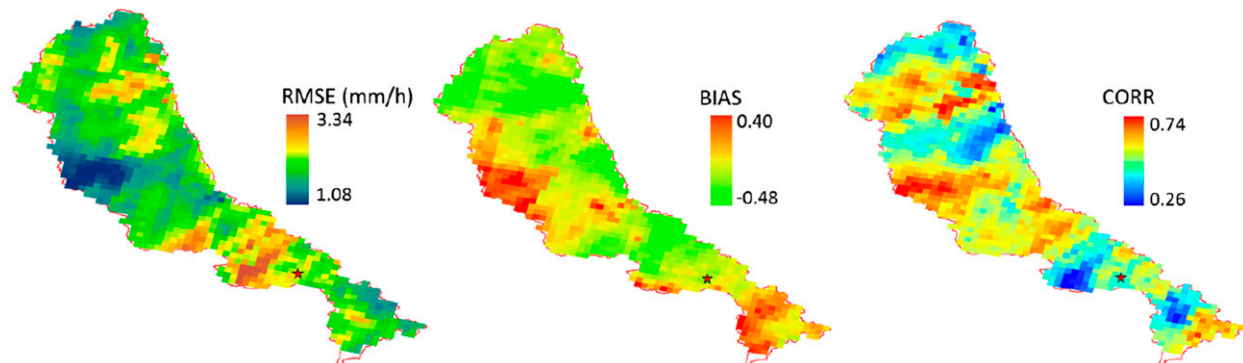


FIG. 5. Comparison statistics between Stage 2 and PERSIANN-CCS hourly precipitation from 0000 UTC 29 May to 2300 UTC 25 Jun 2008: (from left to right) RMSE, BIAS [unitless, calculated from Eq. (5)], and CORR.

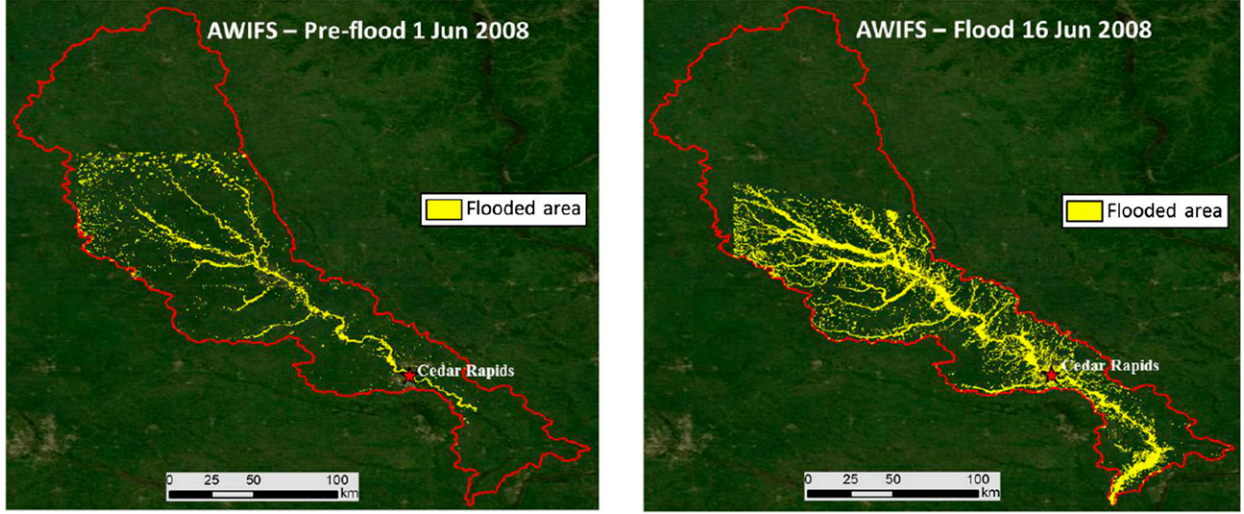


FIG. 6. AWIFS images of preflood (1 Jun 2008) and flood (16 Jun 2008) from USDA.

product depicts flooded areas that are noisy and disconnected from the main channel. While these classifications may be correct (i.e., small ponds), both the preflood and postflood images were manually cleaned such that only pixels of the main river channel and its tributaries were left. This allows for a more straightforward analysis of the model's performance of flooding the actual river by negating any influence the isolated ponds (not connected to the main river) would have on performance metrics.

c. Performance metrics

The AWIFS areal imagery of flood inundation was used to validate the results from the model. The predicted flooded maps were interpolated into 56-m resolution regular grid in order to be spatially compared with the AWIFS images.

Three metrics—probability of detection (POD), false alarm ratio (FAR), and critical success index (CSI)—were used with three statistics (Table 2): hits (having flood in both AWIFS and predicted by HiResFlood-UCI), misses (flooded in AWIFS but not in HiResFlood-UCI), and false alarms (not flooded in AWIFS but flooded in HiResFlood-UCI).

Using the statistics of hits, misses, and false alarms in Table 2, the POD, FAR, and CSI were calculated similarly to Gourley et al. (2012):

$$\text{POD} = \frac{\text{hits}}{\text{hits} + \text{misses}}, \quad (1)$$

$$\text{FAR} = \frac{\text{false alarms}}{\text{hits} + \text{false alarms}}, \quad (2)$$

and

$$\text{CSI} = \frac{\text{hits}}{\text{hits} + \text{misses} + \text{false alarms}}. \quad (3)$$

The model-predicted results were also compared with the USGS's hourly observed streamflow at the gauges along the river network using three common metrics: RMSE, BIAS, and Pearson correlation coefficient (CORR). RMSE, BIAS, and CORR were computed:

$$\text{RMSE} = \sqrt{\frac{1}{n} \sum_{i=1}^n (q_{o,i} - q_{s,i})^2}, \quad (4)$$

$$\text{BIAS} = \frac{\sum_{i=1}^n (q_{s,i} - q_{o,i})}{\sum_{i=1}^n q_{o,i}}, \quad (5)$$

and

$$\text{CORR} = \frac{\sum_{i=1}^n (q_{o,i} - \bar{q}_o) \sum_{i=1}^n (q_{s,i} - \bar{q}_s)}{\sqrt{\sum_{i=1}^n (q_{o,i} - \bar{q}_o)^2} \sqrt{\sum_{i=1}^n (q_{s,i} - \bar{q}_s)^2}}, \quad (6)$$

where n is the total number of observations, q_o is the observed discharge ($\text{m}^3 \text{s}^{-1}$), q_s is the simulated discharge

TABLE 2. Contingency table used in flooded map validation.

		AWIFS image	
		Flooded	Not flooded
Predicted by HiResFlood-UCI	Flooded	Hit	False alarm
	Not flooded	Miss	—

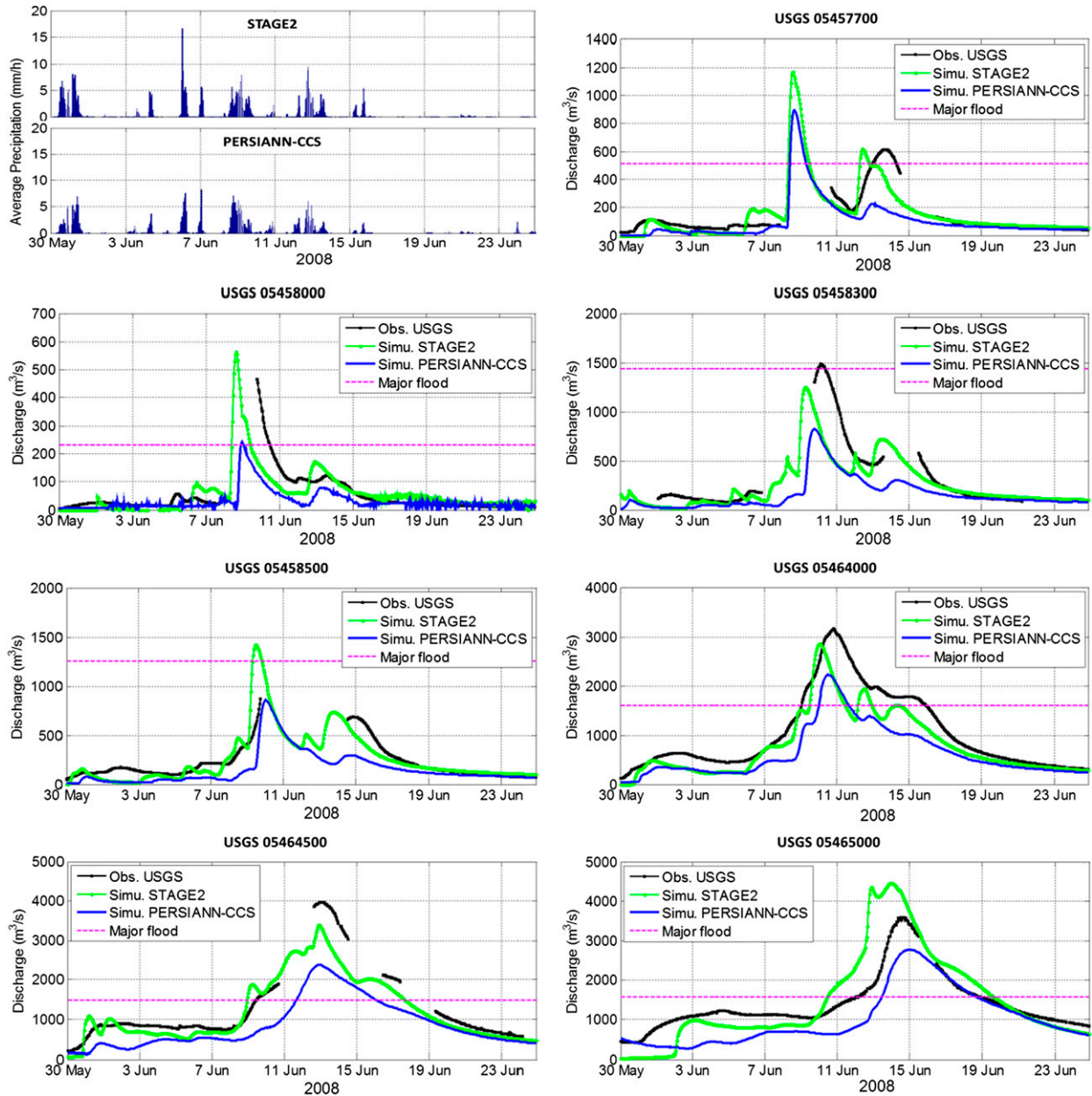


FIG. 7. (top left) Average precipitation. (top right and below) USGS observed hydrographs and model results from model with Stage 2 and PERSIANN-CCS precipitation data.

($\text{m}^3 \text{s}^{-1}$) for each time step i , \bar{q}_o is the mean of the observed values, and \bar{q}_s is the mean of the predicted values.

d. Results and discussion

1) STREAMFLOW VALIDATION

Figure 7 shows the simulated and observed hydrographs at each of the seven USGS gauge locations in the Cedar River basin during the 2008 Iowa flood event. Hourly basin average precipitation as captured by Stage

2 radar and PERSIANN-CCS is also highlighted in Fig. 7. The major flood level at each gauge location as defined by the NWS is plotted as well. In general, both simulations replicate the observed streamflow well in terms of event timing, but struggle in terms of peak magnitude. The PERSIANN-CCS simulation catches the general shape of the observed streamflow, as evidenced by high correlation values in Table 3, but underestimates flow magnitude overall. On the other hand, the Stage 2 simulation overestimates peak magnitude at

TABLE 3. Statistics of event simulations with Stage 2 and PERSIANN-CCS precipitation data comparing with USGS observed streamflow.

USGS streamflow gauge	Precipitation input	RMSE ($\text{m}^3 \text{s}^{-1}$)	BIAS	CORR
05457700	Stage 2	77.79	-0.08	0.85
	PERSIANN-CCS	119.84	-0.51	0.87
05458000	Stage 2	46.50	-0.14	0.72
	PERSIANN-CCS	54.06	-0.50	0.87
05458300	Stage 2	233.32	-0.28	0.87
	PERSIANN-CCS	256.97	-0.48	0.97
05458500	Stage 2	139.07	-0.05	0.79
	PERSIANN-CCS	151.43	-0.54	0.86
05464000	Stage 2	353.32	-0.22	0.94
	PERSIANN-CCS	493.58	-0.39	0.99
05464500	Stage 2	328.10	-0.13	0.96
	PERSIANN-CCS	631.54	-0.42	0.97
05465000	Stage 2	609.22	0.05	0.91
	PERSIANN-CCS	518.85	-0.30	0.89

some locations while underestimating at others and features sharper, more frequent peaks than the observation and the PERSIANN-CCS simulation.

Statistics in Table 3 highlight the differences in hydrographs produced throughout the basin when using Stage 2 radar data versus PERSIANN-CCS data as they compare to observed USGS streamflow gauge measurements. RMSE values between the two simulations are comparable, but the Stage 2 simulation has a lower RMSE than the PERSIANN-CCS simulation at all gauges, except at the outlet. In nearly all of the cases, simulations using Stage 2 and PERSIANN-CCS have a negative bias, with the PERSIANN-CCS forced simulation having a larger bias. Since the model was run using a priori parameter grids, it is possible that with calibration, such bias could be reduced. For correlation, both simulations show a strong performance throughout the basin, with the lowest value for either case at 0.72. The PERSIANN-CCS simulation slightly outperformed Stage 2 at all stream gauge locations except at the outlet in terms of correlation. This outcome comes with a caveat in that for many of the stream gauge locations, the Stage 2 simulation exhibits a streamflow magnitude closer to that of the observations for the duration of the period, but it has higher-frequency variability than the PERSIANN-CCS simulation. By the nature of the Pearson correlation coefficient calculation, these higher-frequency variations (even if they are very small in magnitude) will be penalized. In fact, the rise and recession rates during the flood event appear to be better captured in the Stage 2 simulation, even if peak timing tends to be early.

2) INUNDATION MAP VALIDATION

The model not only can provide a step-by-step picture of the flooded conditions, but it can also highlight the

maximum impact (e.g., maximum depth and maximum flow velocity) at each location for an event. Figure 8 is one example of such an image, as it shows the maximum depth experienced during the flood event for the entire basin. Such information is not available from the widely used HL-RDHM, and it is a unique feature of the HiResFlood-UCI. The validation of the model simulation against the AWIFS product is carried out for a flood map at a certain time step. Also highlighted in Fig. 8 is the area that was selected for validation (the “extended” Cedar Rapids area). This area was chosen for its high flood impact and complete AWIFS coverage.

The cleaned, AWIFS imagery-based preflood and flood inundation maps for Cedar Rapids and the surrounding area are shown in Fig. 9. Figure 10 shows the simulated inundation maps of the corresponding area for the Stage 2 and PERSIANN-CCS forced simulations for the flood on 16 June 2008.

Figure 11 shows the hit–miss–false alarm map for the simulations using each precipitation product. Using the AWIFS inundation maps as “truth,” the Stage 2 simulation overestimated the flood extent as exemplified by more false alarm pixels than missed pixels. On the other hand, the PERSIANN-CCS simulation tends to have more misses than the Stage 2 simulation. This is a somewhat expected by-product of PERSIANN-CCS showing less precipitation in the flood event total precipitation map (Fig. 4). In fact, previous satellite validation studies indicate that satellite precipitation datasets tend to underestimate precipitation, especially at higher rain rates (AghaKouchak et al. 2011, 2012). This can explain the underestimation of peak discharge relative to the Stage 2. However, the results show that satellite observations still provide comparable flood estimates and inundation maps.

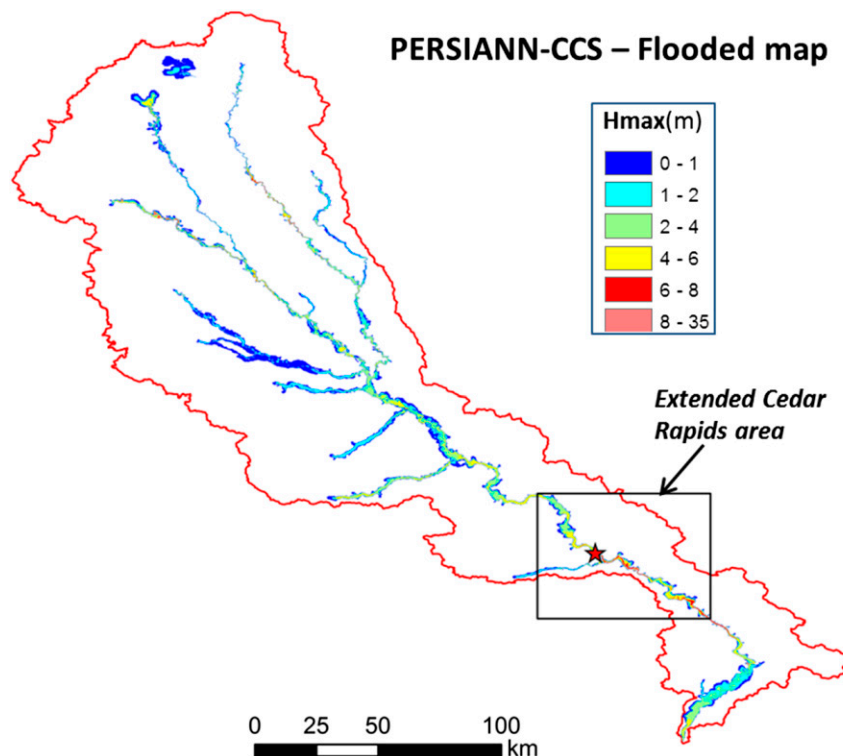


FIG. 8. Max flood depth (m) during the event simulated with PERSIANN-CCS and extended Cedar Rapids area (41.739° – 42.196° N, 91.878° – 91.246° W).

Table 4 summarizes the spatial statistics for both simulations as they relate to the AWIFS maps of the extended Cedar Rapids area. The CSI for the PERSIANN-CCS simulation is slightly higher than the Stage 2 simulation, which suggests it correctly identified flooded pixels with few mistakes (miss or false alarm) compared to the Stage 2 run. Overall, both simulations performed well, as the model was able to capture much of the detail present in the AWIFS-based maps when forced

with both precipitation products. This highlights the value of satellite observations for flood forecasting and inundation mapping in remote regions where radar observations are not available (Sorooshian et al. 2011).

6. Conclusions and future direction

The coupled hydrologic-hydraulic model HiResFlood-UCI was driven by near-real-time remote sensing data in

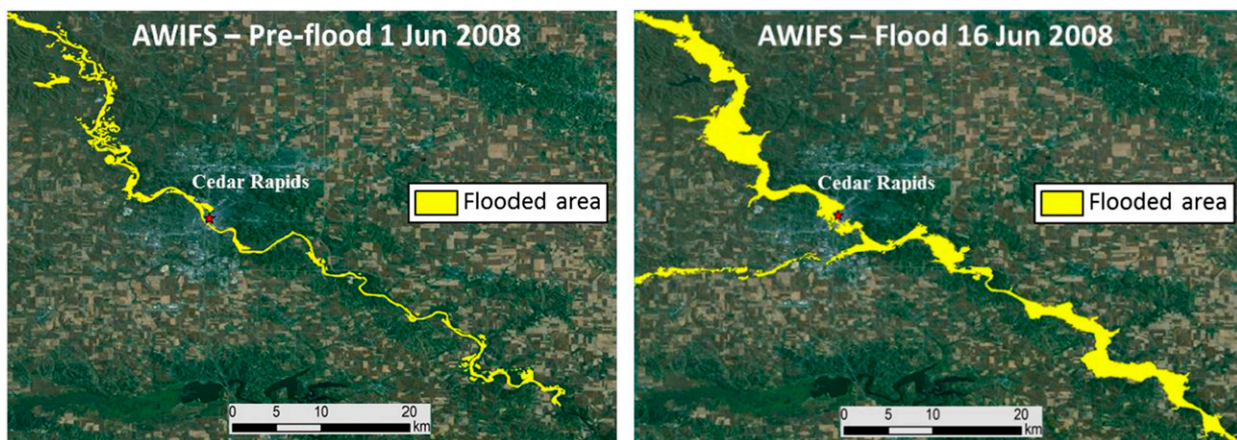


FIG. 9. Cleaned flooded maps of preflood and flood over the extended Cedar Rapids area.

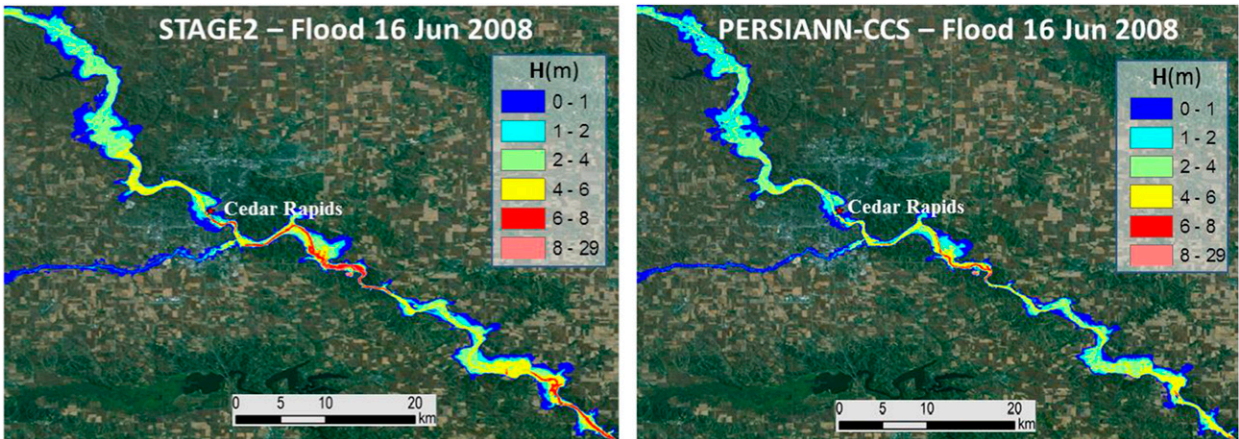


FIG. 10. Modeled flood depth maps with Stage 2 and PERSIANN-CCS precipitation data over the extended Cedar Rapids area.

an effort to demonstrate flood inundation mapping capabilities of the model in a forecasting framework. Two near-real-time precipitation products, PERSIANN-CCS satellite-based product and Stage 2 radar, were used as input for simulating the historic 2008 Iowa flood. This study exploited the rare AWIFS areal imagery of the Cedar River in the extended Cedar Rapids area before and during the flood as a means of validating the model-generated flood extent maps. Basin internal and outlet hydrographs from the model were compared to corresponding observed gauges as a secondary investigation of model performance.

The AWIFS dataset of inundation extent for the 2008 Iowa flood event allowed for a unique experimental setup that encompasses three varieties of remote sensing for either simulation or validation. With AWIFS imagery as a baseline, simulations forced by both Stage 2 and PERSIANN-CCS produced flood maps of the extended Cedar Rapids area with high PODs (0.97 and 0.93, respectively).

Streamflow gauges located at basin interior points reveal high streamflow correlations with both simulations, with a minimum correlation of 0.72 for the Stage 2 simulation and 0.86 for the PERSIANN-CCS simulation. The Stage 2 simulation tends to replicate event magnitude better than the PERSIANN-CCS run, as evidenced by a 42%–90% bias reduction from PERSIANN-CCS to Stage 2. The PERSIANN-CCS simulation captures the observed hydrograph shape more accurately, which is also supported by the PERSIANN-CCS run's higher correlation coefficients and better peak timing. However, because of the sharper, more frequent peaks exhibited in the Stage 2 runs, it is expected that it would have slightly lower correlation coefficients despite showing more representative rise and recession rates.

Through application of the newly developed HiResFlood-UCI, paired with near-real-time, remotely sensed precipitation data, this study demonstrates the ability to recreate detailed flood information

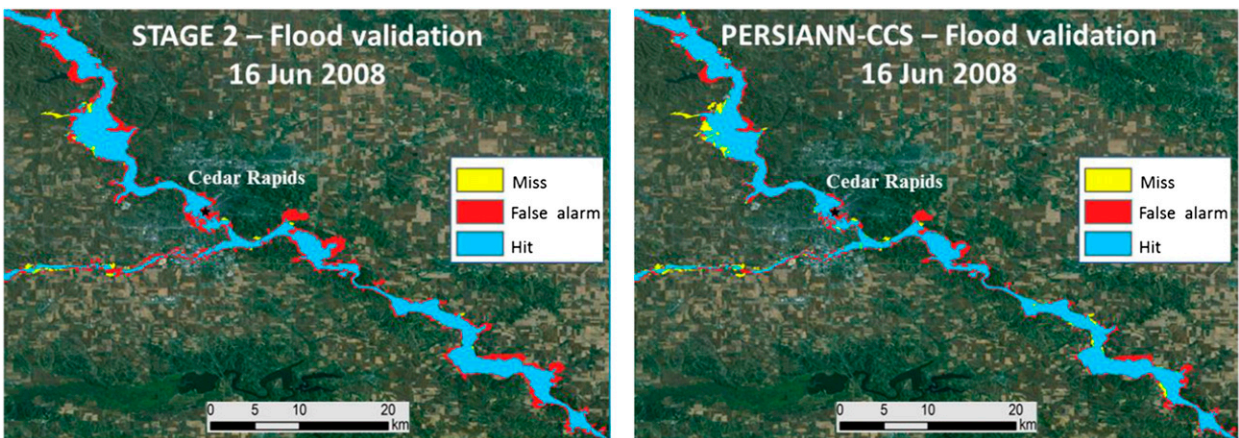


FIG. 11. Validations of flooded maps from the model (with Stage 2 and PERSIANN-CCS precipitation) using AWIFS areal imagery.

TABLE 4. Statistics of flooded map validations for the extended Cedar Rapids area.

Precipitation input	CSI	POD	FAR
Stage 2	0.67	0.97	0.31
PERSIANN-CCS	0.73	0.93	0.23

(particularly flood extent maps) in a forecasting setting. Strong simulation performance for this application is particularly promising, given the fact that the HiResFlood-UCI was run with a priori parameters provided by the NWS. Validation of the event via unique aerial imagery available pre- and postflood and observed hydrographs reinforces trust in the modeled results. This study investigates the use of two fundamentally different precipitation estimation products in flood forecasting. In doing so, early components of an ensemble-based forecasting system have been introduced and provide an opportunity for future development. This approach may lead to probabilistic inundation predictions that incorporate uncertainties present in precipitation estimation products.

Largely, results from this work demonstrate the potential benefits to society, especially in regions with poorly monitored data. Simulation of a data-rich basin using information and tools available globally permits the evaluation of the type of results that could be expected in a region where the critical calibration/validation step is nearly impossible.

Acknowledgments. This research was supported by the NOAA Office of Hydrologic Development (OHD) National Weather Service (NWS) student research fellowship and the Department of Defense (DoD) through the National Defense Science and Engineering Graduate Fellowship (NDSEG) Program. This work was also supported by the Cooperative Institute for Climate and Satellites (CICS) and the Army Research Office (Award W911NF-11-1-0422). The first author was financially supported by the Vietnamese International Education Development program and the University of California, Irvine, Chancellor Club for Excellence Fellowship while conducting this research. We would like to acknowledge high-performance computing support from Yellowstone (ark:/85065/d7wd3xhc) provided by NCAR's Computational and Information Systems Laboratory, sponsored by the National Science Foundation. Stage 2 rainfall data were provided by NCAR/EOL under sponsorship of the National Science Foundation (<http://data.eol.ucar.edu/>).

REFERENCES

- AghaKouchak, A., A. Behrang, S. Sorooshian, K. Hsu, and E. Amitai, 2011: Evaluation of satellite-retrieved extreme precipitation rates across the central United States. *J. Geophys. Res.*, **116**, D02115, doi:[10.1029/2010JD014741](https://doi.org/10.1029/2010JD014741).
- , A. Mehran, H. Norouzi, and A. Behrang, 2012: Systematic and random error components in satellite precipitation data sets. *Geophys. Res. Lett.*, **39**, L09406, doi:[10.1029/2012GL051592](https://doi.org/10.1029/2012GL051592).
- Alsdorf, D. E., E. Rodriguez, and D. P. Lettenmaier, 2007: Measuring surface water from space. *Rev. Geophys.*, **45**, RG2002, doi:[10.1029/2006RG000197](https://doi.org/10.1029/2006RG000197).
- Ashley, S., and W. Ashley, 2008: Flood fatalities in the United States. *J. Appl. Meteor. Climatol.*, **47**, 806–818, doi:[10.1175/2007JAMC1611.1](https://doi.org/10.1175/2007JAMC1611.1).
- Bates, P. D., M. S. Horritt, C. N. Smith, and D. Mason, 1997: Integrating remote sensing observations of flood hydrology and hydraulic modelling. *Hydrol. Processes*, **11**, 1777–1795, doi:[10.1002/\(SICI\)1099-1085\(199711\)11:14<1777::AID-HYP543>3.0.CO;2-E](https://doi.org/10.1002/(SICI)1099-1085(199711)11:14<1777::AID-HYP543>3.0.CO;2-E).
- Begnudelli, L., and B. F. Sanders, 2006: Unstructured grid finite-volume algorithm for shallow-water flow and scalar transport with wetting and drying. *J. Hydraul. Eng.*, **132**, 371–384, doi:[10.1061/\(ASCE\)0733-9429\(2006\)132:4\(371\)](https://doi.org/10.1061/(ASCE)0733-9429(2006)132:4(371)).
- , and —, 2007: Conservative wetting and drying methodology for quadrilateral grid finite volume models. *J. Hydraul. Eng.*, **133**, 312–322, doi:[10.1061/\(ASCE\)0733-9429\(2007\)133:3\(312\)](https://doi.org/10.1061/(ASCE)0733-9429(2007)133:3(312)).
- Behrang, A., B. Khakbaz, T. C. Jaw, A. AghaKouchak, K. Hsu, and S. Sorooshian, 2011: Hydrologic evaluation of satellite precipitation products over a mid-size basin. *J. Hydrol.*, **397**, 225–237, doi:[10.1016/j.jhydrol.2010.11.043](https://doi.org/10.1016/j.jhydrol.2010.11.043).
- Bjerkli, D. M., D. Moller, L. C. Smith, and S. L. Dingman, 2005: Estimating discharge in rivers using remotely sensed hydraulic information. *J. Hydrol.*, **309**, 191–209, doi:[10.1016/j.jhydrol.2004.11.022](https://doi.org/10.1016/j.jhydrol.2004.11.022).
- Borga, M., E. N. Anagnostou, G. Bloschl, and J. D. Creutin, 2011: Flash flood forecasting, warning and risk management: The HYDRATE project. *Environ. Sci. Policy*, **14**, 834–844, doi:[10.1016/j.envsci.2011.05.017](https://doi.org/10.1016/j.envsci.2011.05.017).
- Boryan, C., Z. Yang, R. Mueller, and M. Craig, 2011: Monitoring US agriculture: The US Department of Agriculture, National Agricultural Statistics Service, Cropland Data Layer Program. *Geocarto Int.*, **26**, 341–358, doi:[10.1080/10106049.2011.562309](https://doi.org/10.1080/10106049.2011.562309).
- Brakenridge, G. R., S. V. Nghiem, E. Anderson, and R. Mic, 2007: Orbital microwave measurement of river discharge and ice status. *Water Resour. Res.*, **43**, W04405, doi:[10.1029/2006WR005238](https://doi.org/10.1029/2006WR005238).
- Chow, V. T., 1959: *Open-Channel Hydraulics*. McGraw-Hill, 680 pp.
- Collier, C. G., 2007: Flash flood forecasting: What are the limits of predictability? *Quart. J. Roy. Meteor. Soc.*, **133**, 3–23, doi:[10.1002/qj.29](https://doi.org/10.1002/qj.29).
- Cook, A., and V. Merwade, 2009: Effect of topographic data, geometric configuration and modeling approach on flood inundation mapping. *J. Hydrol.*, **377**, 131–142, doi:[10.1016/j.jhydrol.2009.08.015](https://doi.org/10.1016/j.jhydrol.2009.08.015).
- Gourley, J. J., J. M. Erlingis, Y. Hong, and E. Wells, 2012: Evaluation of tools used for monitoring and forecasting flash floods in the United States. *Wea. Forecasting*, **27**, 158–173, doi:[10.1175/WAF-D-10-05043.1](https://doi.org/10.1175/WAF-D-10-05043.1).
- Hong, Y., K. Hsu, S. Sorooshian, and X. Gao, 2004: Precipitation estimation from remotely sensed imagery using an artificial neural network cloud classification system. *J. Appl. Meteor.*, **43**, 1834–1852, doi:[10.1175/JAM2173.1](https://doi.org/10.1175/JAM2173.1).
- , R. F. Adler, A. Negri, and G. J. Huffman, 2007a: Flood and landslide applications of near real-time satellite rainfall products. *Nat. Hazards*, **43**, 285–294, doi:[10.1007/s11069-006-9106-x](https://doi.org/10.1007/s11069-006-9106-x).

- , D. Gochis, J. T. Chen, K. L. Hsu, and S. Sorooshian, 2007b: Evaluation of PERSIANN-CCS rainfall measurement using the NAME event rain gauge network. *J. Hydrometeor.*, **8**, 469–482, doi:[10.1175/JHM574.1](https://doi.org/10.1175/JHM574.1).
- Hossain, F., A. H. Siddique-E-Akbor, L. C. Mazumder, S. M. ShahNewaz, S. Biancamaria, H. Lee, and C. K. Shum, 2014a: Proof of concept of an altimeter-based river forecasting system for transboundary flow inside Bangladesh. *IEEE J. Sel. Topics Appl. Earth Obs. Remote Sens.*, **7**, 587–601, doi:[10.1109/JSTARS.2013.2283402](https://doi.org/10.1109/JSTARS.2013.2283402).
- , and Coauthors, 2014b: Crossing the “Valley of Death”: Lessons learned from implementing an operational satellite-based flood forecasting system. *Bull. Amer. Meteor. Soc.*, **95**, 1201–1207, doi:[10.1175/BAMS-D-13-00176.1](https://doi.org/10.1175/BAMS-D-13-00176.1).
- Hsu, K., X. Gao, S. Sorooshian, and H. V. Gupta, 1997: Precipitation estimation from remotely sensed information using artificial neural networks. *J. Appl. Meteor.*, **36**, 1176–1190, doi:[10.1175/1520-0450\(1997\)036<1176:PEFRSI>2.0.CO;2](https://doi.org/10.1175/1520-0450(1997)036<1176:PEFRSI>2.0.CO;2).
- , S. Sellars, P. Nguyen, D. Braithwaite, and W. Chu, 2013: G-WADI PERSIANN-CCS GeoServer for extreme precipitation event monitoring. *Sci. Cold Arid Reg.*, **5** (1), 6–15.
- Indian National Remote Sensing Agency, 2003: IRS-P6 data user’s manual. 141 pp. [Available online at www.euromap.de/download/P6_data_user_handbook.pdf.]
- Jensen, J. R., 2000: *Remote Sensing of the Environment: An Earth Resource Perspective*. Prince Hall, 544 pp.
- Johnson, D., and M. Lindsey, 2008: AWiFS data: Helping reinforce crop acreage statistics within June 2008’s flooded areas. *Integrating ResourceSat-LISS and AWiFS Data into Multi-Sensor Solutions Seminar*, Greenbelt, MD, USDA. [Available online at www.nass.usda.gov/Education_and_Outreach/Reports_Presentations_and_Conferences/Presentations/Johnson_FASSeminar08.pdf.]
- Khan, S. I., Y. Hong, J. J. Gourley, M. U. Khattak, and T. D. Groeve, 2014: Multi-sensor imaging and space-ground cross-validation for 2010 flood along Indus River, Pakistan. *Remote Sens.*, **6**, 2393–2407, doi:[10.3390/rs6032393](https://doi.org/10.3390/rs6032393).
- Koren, V., M. Smith, and Q. Duan, 2003: Use of a priori parameter estimates in the derivation of spatially consistent parameter sets of rainfall-runoff models. *Calibration of Watershed Models*, Q. Duan et al., Eds., Water Science and Application Series, Vol. 6, Amer. Geophys. Union, 239–254, doi:[10.1002/9781118665671.ch18](https://doi.org/10.1002/9781118665671.ch18).
- , S. Reed, M. Smith, Z. Zhang, and D. J. Seo, 2004: Hydrology laboratory modeling system (HL-RMS) of the US national weather service. *J. Hydrol.*, **291**, 297–318, doi:[10.1016/j.jhydrol.2003.12.039](https://doi.org/10.1016/j.jhydrol.2003.12.039).
- Krajewski, W., B. C. Seo, R. Goska, I. Demir, and M. Elsaadani, 2013: Precipitation datasets the GPM Iowa Flood Studies (IFloodS) field experiment. *Geophysical Research Abstracts*, Vol. 15, Abstract EGU2013-11303. [Available online at <http://meetingorganizer.copernicus.org/EGU2013/EGU2013-11303.pdf>.]
- Linhart, S. M., and D. A. Eash, 2010: Floods of May 30 to June 15, 2008, in the Iowa River and Cedar River basins, eastern Iowa. USGS Open-File Rep. 2010-1190, 99 pp. [Available online at <http://pubs.usgs.gov/of/2010/1190/pdf/of2010-1190.pdf>.]
- National Weather Service, 2011: Hydrology Laboratory-Research Distributed Hydrologic Model (HL-RDHM) User Manual V. 3.2.0. National Weather Service Rep., 79 pp.
- , 2012: Summary of Natural Hazard Statistics for 2011 in the United States. Accessed 10 September 2014. [Available online at www.nws.noaa.gov/os/hazstats/sum11.pdf.]
- Nguyen, P., S. Sorooshian, K. Hsu, A. AghaKouchak, B. Sanders, M. Smith, and V. Koren, 2012: Improving flash flood forecasting through coupling of a distributed hydrologic rainfall-runoff model (HL-RDHM) with a hydraulic model (BreZo). *2012 Fall Meeting*, San Francisco, CA, Amer. Geophys. Union, Abstract H43F-1429. [Available online at <http://fallmeeting.agu.org/2012/eposters/eposter/h43f-1429/>.]
- , —, —, —, and —, 2013: Modeling the Upper Little Missouri River flash flood 2010 using a coupled distributed hydrologic-hydraulic model. *CSDMS Annual Meeting 2013*, Boulder, CO, CSDMS. [Available online at http://csdms.colorado.edu/mediawiki/images/CSDMS2013_poster_PhuNguyen.pdf.]
- , S. Sellars, A. Thorstensen, Y. Tao, H. Ashouri, D. Braithwaite, K. Hsu, and S. Sorooshian, 2014: Satellites Track Precipitation of Super Typhoon Haiyan. *Eos, Trans. Amer. Geophys. Union*, **95**, 133–135, doi:[10.1002/2014EO160002](https://doi.org/10.1002/2014EO160002).
- Sanders, B. F., 2007: Evaluation of on-line DEMs for flood inundation modeling. *Adv. Water Resour.*, **30**, 1831–1843, doi:[10.1016/j.advwatres.2007.02.005](https://doi.org/10.1016/j.advwatres.2007.02.005).
- Shewchuk, J. R., 1996: Triangle: Engineering a 2D quality mesh generator and Delaunay triangulator. *Lect. Notes Comput. Sci.*, **1148**, 203–222, doi:[10.1007/BFb0014497](https://doi.org/10.1007/BFb0014497).
- Smith, J. A., M. L. Baeck, G. Villarini, D. B. Wright, and W. Krajewski, 2013: Extreme flood response: The June 2008 flooding in Iowa. *J. Hydrometeor.*, **14**, 1810–1825, doi:[10.1175/JHM-D-12-0191.1](https://doi.org/10.1175/JHM-D-12-0191.1).
- Solomon, S., D. Qin, M. Manning, Z. Chen, M. Marquis, K. Averyt, M. Tignor, and H. L. Miller Jr., Eds., 2007: *Climate Change 2007: The Physical Science Basis*. Cambridge University Press, 996 pp.
- Sorooshian, S., K. Hsu, X. Gao, H. Gupta, B. Imam, and D. Braithwaite, 2000: Evaluation of PERSIANN system satellite-based estimates of tropical rainfall. *Bull. Amer. Meteor. Soc.*, **81**, 2035–2046, doi:[10.1175/1520-0477\(2000\)081<2035:EOPSS>2.3.CO;2](https://doi.org/10.1175/1520-0477(2000)081<2035:EOPSS>2.3.CO;2).
- , and Coauthors, 2011: Advanced concepts on remote sensing of precipitation at multiple scales. *Bull. Amer. Meteor. Soc.*, **92**, 1353–1357, doi:[10.1175/2011BAMS3158.1](https://doi.org/10.1175/2011BAMS3158.1).
- , P. Nguyen, S. Sellars, D. Braithwaite, A. AghaKouchak, and K. Hsu, 2014: Satellite-based remote sensing estimation of precipitation for early warning systems. *Extreme Natural Hazards, Disaster Risks and Societal Implications*, A. Ismail-Zadeh et al., Eds., Special Publications of the International Union of Geodesy and Geophysics, No. 1, Cambridge University Press, 99–112, doi:[10.1017/CBO9781139523905.011](https://doi.org/10.1017/CBO9781139523905.011).
- WMO, 2011: Manual on flood forecasting and warning. WMO Rep. 1072, 140 pp. [Available online at www.wmo.int/pages/prog/hwrp/publications/flood_forecasting_warning/WMO%201072_en.pdf.]
- Wu, H., R. F. Adler, Y. Tian, G. J. Huffman, H. Li, and J. Wang, 2014: Real-time global flood estimation using satellite-based precipitation and a coupled land surface and routing model. *Water Resour. Res.*, **50**, 2693–2717, doi:[10.1002/2013WR014710](https://doi.org/10.1002/2013WR014710).